

# X-ray emission from BH+O star binaries expected to descend from the observed galactic WR+O binaries

K. Sen<sup>1,2</sup> \*, X.-T. Xu<sup>1,2</sup> \*\*, N. Langer<sup>1,2</sup>, I. El Mellah<sup>3</sup>, C. Schürmann<sup>1,2</sup>, and M. Quast<sup>1</sup>

<sup>1</sup> Argelander-Institut für Astronomie, Universität Bonn, Auf dem Hugel 71, 53121 Bonn, Germany

<sup>2</sup> Max-Planck-Institut für Radioastronomie, Auf dem Hugel 69, 53121 Bonn, Germany

<sup>3</sup> Univ. Grenoble Alpes, CNRS, IPAG, 414 Rue de la Piscine, 38400 Saint-Martin-d'Hères, France

Received June 4, 2021/ Accepted ...

## ABSTRACT

**Context.** In the Milky Way, ~18 Wolf-Rayet+O star (WR+O) binaries are known with estimates of their stellar and orbital parameters. Whereas black hole+O star (BH+O) binaries are thought to evolve from WR+O binaries, only one such system is known in the Milky Way. To resolve this disparity, it was suggested recently that upon core collapse, the WR stars receive large kicks such that most of the binaries are disrupted.

**Aims.** We reassess this issue, with particular emphasis on the uncertainty in predicting the X-ray emission from wind-accreting BHs in BH+O binaries, which is key to identifying such systems.

**Methods.** BH+O systems are thought to be X-ray bright only when an accretion disk forms around the BHs. We follow the methodology of previous work and apply an improved analytic criterion for the formation of an accretion disk around wind accreting BHs. We then use stellar evolutionary models to predict the properties of the BH+O binaries which are expected to descend from the observed WR+O binaries if the WR stars would form BHs without a natal kick.

**Results.** We find that disk formation depends sensitively on the O stars' wind velocity, the amount of specific angular momentum carried by the wind, the efficiency of angular momentum accretion by the BH, and the spin of the BH. We show that whereas the assumption of a low wind velocity may lead to the prediction that most of the BH+O star binaries will have an extended X-ray bright period, this is not the case when typical wind velocities of O stars are considered. We find that a high spin of the BH can boost the duration of the X-ray active phase as well as the X-ray brightness during this phase. This produces a strong bias for detecting high mass BH binaries in X-rays with high BH spin parameters.

**Conclusions.** We find that large BH formation kicks are not required to understand the sparsity of X-ray bright BH+O stars in the Milky Way. Probing for a population of X-ray silent BH+O systems with alternative methods can likely inform us about BH kicks and the necessary conditions for high energy emission from high mass BH binaries.

**Key words.** Stars: massive – Stars: evolution – Stars: black holes – X-rays: binaries – (Stars) binaries: close

## 1. Introduction

The detection of gravitational waves by LIGO/VIRGO in the last decade has opened a new window to look at our Universe. Since the first observation by LIGO in 2015 (Abbott et al. 2016, 2019), most of these, now routine, events are associated with merging stellar mass black holes (Abbott et al. 2019). Thereby, the interest in the study of black holes has been revitalised (de Mink & Mandel 2016; Marchant et al. 2016; Belczynski et al. 2020; Woosley et al. 2020; du Buisson et al. 2020). But the evolution of massive star binaries towards binary compact object mergers is still riddled with uncertainties (Langer 2012; Crowther 2019).

Apart from gravitational wave signals from compact object mergers and direct imaging of the supermassive BH shadows (Event Horizon Telescope Collaboration et al. 2019), BHs can be detected via microlensing (Minniti et al. 2015; Masuda & Hotokezaka 2019; Wyrzykowski & Mandel 2020), tidal disruption events (Perets et al. 2016; Kremer et al. 2019), and X-ray emission due to accretion onto the BH. In the latter case, the source of material can be dense interstellar medium (Fujita et al. 1998;

Tsuna et al. 2018; Scarcella et al. 2020), or an orbiting stellar companion (Orosz et al. 2011).

A large number of binary population synthesis studies have been undertaken to predict the event rate of merging compact objects (Mennekens & Vanbeveren 2014; Belczynski et al. 2014; Stevenson et al. 2015; de Mink & Belczynski 2015; Kruckow et al. 2018). One of the major uncertainties in population synthesis studies (for a discussion, see O'Shaughnessy et al. 2008) is whether the formation of a BH is preceded by a SN explosion and if so, whether the BH receives a natal kick high enough to disrupt the binary in which the BH formed (Mandel & Müller 2020; Mandel et al. 2021; Woosley et al. 2020). As expected, the presence or absence of a substantial kick during BH formation significantly affects the BH-BH merger rates calculated by population synthesis calculations (Mennekens & Vanbeveren 2014; Belczynski et al. 2016).

Direct evidence towards high or low BH kicks is inconclusive (Özel et al. 2010; Farr et al. 2011; Belczynski et al. 2012). On one hand, in Galactic low mass X-ray binaries containing a BH, BHs were found to have formed with low or modest kick velocities (Brandt et al. 1995; Willems et al. 2005; Fragos et al. 2009; Wong et al. 2012). Belczynski et al. (2016) (table 7, and references therein) have given empirical evidence for low BH

\* email: ksen@astro.uni-bonn.de

\*\* The first two authors have contributed equally to this work

natal kicks. On the other hand, Repetto et al. (2012, 2017) found that their binary models can adequately explain the observed population of low mass BH binaries above the Galactic plane when high BH kick velocities, similar to the ones assumed for the formation of neutron stars (Hobbs et al. 2005), are adopted during BH formation. Moreover, some works have suggested a BH mass dependent natal kick distribution (Mirabel & Rodrigues 2003; Dhawan et al. 2007), with more massive BHs receiving lower kicks.

Several teams have studied whether very massive stars can explode at the end of their lifetime (O’Connor & Ott 2011; Ugliano et al. 2012). Sukhbold et al. (2018) and Woosley (2019) predict that most of the hydrogen free Helium stars having masses between 7-30  $M_{\odot}$ , which will also manifest as Wolf-Rayet stars during helium burning, do not explode with an associated supernova but instead implode into BHs. Mirabel & Rodrigues (2003) show evidence that WR stars might become BHs with little or no kick.

Langer et al. (2020) predicted to find  $\sim 3$  out of every 100 massive binary stars to host a BH. The average lifetime of the WR+O phase ( $\sim 0.4$  Myrs, given by the lifetime of the WR phase) is much smaller than the lifetime of the BH+O phase (which is given by the remaining main sequence lifetime of the O star). Hence, if the transition from the WR+O stage to the BH+O stage happens without disruption of the binary, we expect the Milky Way to host more binaries containing BHs than WR stars. But the observed number of WR+O star binaries are much larger than BH+O star binaries.

Vanbeveren et al. (2020) (hereafter V20) assessed this problem with the following two assumptions: (i) WR stars collapse to form BHs with no natal kick, (ii) a BH+O binary is detectable if the BH has an accretion disk and the X-ray flux emitted from the accretion disk is above the detection threshold of current X-ray telescopes. They predicted to find over 200 wind-fed BH high mass X-ray Binaries (HMXBs) in the Milky Way. There is only one observed in the Milky Way (Cygnus X-1, see e.g. Hirsch et al. 2019).

The large discrepancy between the predicted and observed number of wind-fed BH HMXBs led V20 to conclude that most of the WR stars must explode in a supernova to form neutron stars with an associated large natal kick that disrupts the binaries, or BH formation itself is associated with a high kick velocity that disrupts most of the progenitor WR+O binaries at the time of BH formation. This conclusion would greatly affect the merger rates of BH-BH and BH-NS mergers as many population synthesis results assume low kick velocities for BH formation.

In this work, we follow Shapiro & Lightman (1976) to formulate a condition for the formation of accretion disks and detectability of a BH+O system as a wind-fed BH HMXB. We investigate the effect of the stellar wind velocity, efficiency of angular momentum accretion from the stellar wind and the spin of the BH, on our prediction of the number of wind-fed BH HMXBs. We also revisit the assumptions and definitions of stellar parameters used to derive the accretion disk formation criterion in the work of V20.

In Sect. 2, we outline the definitions and assumptions used to derive our accretion disk formation criterion. We then predict the population of BH+O binaries and study the effect of uncertain parameters on our predictions in Sect. 3. We compare the assumptions and results in our work with the literature in Sect. 4. In Sect. 5, we critically discuss the implications of the uncertainties that are present in the calculation of the X-ray active lifetime of BH+O binaries and outline our main conclusions from this work in Sect. 6.

**Table 1.** Stellar parameters of the anticipated BH+O binaries obtained by V20 at BH formation, in order of increasing orbital period. The BH is assumed to be formed at the end of core helium depletion of the WR star in the progenitor WR+O binaries.

Progenitor System	distance (kpc)	O star mass ( $M_{\odot}$ )	BH mass ( $M_{\odot}$ )	Orbital period (days)	$L/L_{\text{Edd}}$ of O star
WR 155	2.99	30	12	2.6	0.161
WR 151	5.38	28	10	3.4	0.076
WR 139	1.31	28	6	5.0	0.101
WR 31	6.11	24	7	6.1	0.140
WR 42	2.44	27	14	8.7	0.156
WR 47	3.49	47	20	10.5	0.317
WR 79	1.37	24	7	10.7	0.076
WR 127	3.09	20	6	11.8	0.076
WR 21	3.99	37	10	11.8	0.341
WR 9	4.57	32	8	15.0	0.299
WR 97	2.15	30	9	18.3	0.304
WR 30	5.09	34	14	20.4	0.303
WR 113	1.80	22	8	35.9	0.054
WR 141	1.92	26	18	43.1	0.076
WR 35a	5.84	19	10	68.2	0.054
WR 11	0.34	31	8	86.8	0.107
WR 133	1.85	34	9	158.0	0.107

## 2. Method

### 2.1. Sample selection

In the Milky Way, there are about  $\sim 53$  observed WR+O type binaries<sup>1</sup> (van der Hucht 2001, 2006; Crowther 2015; Rosslowe & Crowther 2015). Of them, 38 are designated as double-lined spectroscopic binaries (SB2). V20 consider a sub-population of 17 SB2 binaries that have estimates of the masses of both components and orbital period of the binary. The present masses of both components and the orbital period of the selected sample of 17 binaries can be found in table 1 of V20. We find one more SB2 system, WR 22, that has estimates of its component masses and orbital period (Schweickhardt et al. 1999). This system has an orbital period around  $\sim 80$  days. In this work, we further look at the distance of the systems from Earth using the catalogue of galactic WR stars (Rosslowe & Crowther 2015) (Table 1). To be consistent with the analysis of V20, we choose to analyse the sub-sample of the 17 WR+O binaries. We also explain later that the addition of WR 22 to the sample of 17 SB2 binaries reinforces the conclusions we derive from our work.

The orbital period distribution of WR+O binaries in the Large Magellanic Cloud is expected to peak at  $\sim 100$  days (Langer et al. 2020), which can be expected to be similar in the Milky Way. Observationally, short period WR+O star binaries are much easier to detect than long period ones. This implies that the sub-sample of  $\sim 17$  mostly short period WR+O binaries considered in this work may indeed account for nearly all short period WR+O binaries expected for the  $\sim 53$  WR+O binaries observed in the Milky Way. We will see below that only short period WR+O binaries can manifest as X-ray bright BH+O systems. In this sense, the sub-sample of 17 WR+O binaries can be used as a suitable proxy to analyse the detectability of anticipated BH+O binaries in the Milky Way.

<sup>1</sup> <http://pacrowther.staff.shef.ac.uk/WRcat/index.php>

## 2.2. Binary evolution

We describe the further modelling of the chosen WR+O binaries in the following subsections.

### 2.2.1. WR+O binary evolution up to BH formation

We adopt the stellar and orbital parameters of the anticipated BH+O binaries derived by V20 at the time of BH formation (Table 1). We describe the modelling of the evolution of the WR+O star binaries performed by V20 up to the point of BH formation briefly in the following paragraph.

The orbital periods of the considered WR+O star binaries suggest that most of them did undergo mass transfer in the past, which stripped the hydrogen-rich envelope of the donor stars and the O star companions may have rejuvenated due to accretion (Braun & Langer 1995). The expected masses of the WR stars at core helium depletion were calculated using the evolutionary tracks of hydrogen deficient, post-Roche Lobe overflow, core helium burning star models of Vanbeveren et al. (1998b). For a WR star of the nitrogen sequence (i.e. WN star), the WR star was assumed to be at the beginning of the helium burning. On the other hand, if a WR star was of the carbon sequence (WC star), the calculation was started from the point during core helium burning when helium burning products appear at the stellar surface due to wind mass loss. This assumption neither affects the main results of V20 nor this study (see appendix of V20 for a discussion). Following this evolution, the expected mass of the WR star at the end of core helium burning was calculated. The orbital periods of the WR+O binaries at the end of core helium burning of the WR stars were estimated using the close binary evolutionary models of Vanbeveren et al. (1998a).

At the end of core helium depletion, we assume that the WR stars will directly collapse into BHs of the same mass without any natal kick. It means that we do not account for the binary disruption which might be induced by high natal kicks. We also neglect the changes in orbital separation and eccentricity provoked by natal kicks. We thus expect the number of wind-fed BH HMXBs predicted from our analysis to be an upper limit on the actual number. Below, we test this assumption a posteriori by comparing our predicted number of wind-fed BH HMXBs with observations. We note that a small natal kick may not lead to disruption of the binary but introduce an eccentricity in the orbit that may result in the production of X-ray at periastron passage. In such a case, the X-ray emission is expected to be periodic and active only for a small fraction of the orbital period. Therefore, we do not expect a small natal kick to significantly alter our results.

### 2.2.2. The BH+O phase

After the formation of the BH, the orbital evolution is driven by the mass loss from the O star companion, which reduces the mass of the O star and carries away orbital angular momentum (Quast et al. 2019; El Mellah et al. 2020a). Whether the orbit shrinks or expands depends on the mass ratio and the fraction of wind material escaping from the system (see fig. 10 in El Mellah et al. 2020a). In our case, the ratio of O star masses to BH masses are below 5, and more than ~99% of wind material escapes from the binary (see Fig. A.1). This implies that we can assume that the orbital parameters remain unchanged during the BH+O phase. Considering the fact that most of these systems might have undergone a mass transfer episode in the past, we also assume that the orbit is circular.

We follow the subsequent evolution of the O star companions in the BH+O binaries by interpolating in the massive single star models of Ekström et al. (2012). Due to past mass transfer from the WR progenitors to the O star companions, the O stars can be found to be younger than the age of the binaries, by the process of rejuvenation (Braun & Langer 1995). This is the so-called rejuvenated ages of the O stars. The rejuvenated ages of the O stars were obtained by V20 from their observed mass, spectral type and luminosity class. Here, we estimated the rejuvenated ages of the O stars at the time of BH formation by reproducing V20's results with their assumptions. For the systems not expected to become detectable BH+O binaries by V20, the rejuvenated ages of the O stars at the time of BH formation are set to be zero. This does not affect our results as we also find no X-ray emission from those systems during the BH+O phase. We assume that the BH+O phase lasts until the O stars leave the main sequence or fill their Roche lobes, whichever is earlier. On the other hand, V20 assumed that the BH+O phase lasts until the O stars fill its Roche lobes.

## 2.3. Wind-captured disks during the BH+O phase

Due to the gravitational field of the BH, a fraction of the stellar wind from the O star can be captured by the BH (Illarionov & Sunyaev 1975). As a result, a wind-captured disk may form around the BH (Shapiro & Lightman 1976; Iben & Tutukov 1996). Due to turbulent viscosity produced by instabilities such as the magneto-rotational instability (Balbus & Hawley 1991), accreting material moves inward in an optically thick and geometrically thin accretion disk, in which gravitational energy is efficiently converted into thermal energy, producing X-ray emission (Shakura & Sunyaev 1973).

### 2.3.1. Wind velocity

The O star wind velocity ( $v_{\text{wind}}$ ) at the location of the BH can be approximated as

$$v_{\text{wind}} = v_{\infty} \left(1 - \frac{R_{\text{O}}}{a}\right)^{\beta}, \quad (1)$$

where  $a$  is the orbital separation,  $v_{\infty}$  is the terminal velocity of stellar wind and  $R_{\text{O}}$  is the radius of the O star. For O stars (effective temperature higher than 30 kK), the value of  $\beta$  is 0.8 - 1 (Groenewegen & Lamers 1989; Puls et al. 1996) and the terminal velocity is given by (Vink et al. 2001)

$$v_{\infty} \approx 2.6 v_{\text{esc}}, \quad (2)$$

where  $v_{\text{esc}}$  is the modified escape velocity of O star

$$v_{\text{esc}} = \sqrt{\frac{2GM_{\text{O}}}{R_{\text{O}}}(1 - \Gamma)}, \quad (3)$$

$\Gamma$  is the Eddington factor, and  $M_{\text{O}}$  is the mass of the O star companion.

### 2.3.2. Disk formation

A necessary condition for the formation of a wind-captured disk around a BH is

$$\frac{R_{\text{disk}}}{R_{\text{ISCO}}} > 1, \quad (4)$$

where  $R_{\text{ISCO}}$  is the radius of the innermost stable orbit and  $R_{\text{disk}}$  is the circularisation radius of a Keplerian accretion disk, defined by

$$R_{\text{disk}} = \frac{j^2}{GM_{\text{BH}}}, \quad (5)$$

where  $j$  is the specific angular momentum of the captured wind material,  $G$  is the gravitational constant, and  $M_{\text{BH}}$  is the mass of the BH. The radius of the innermost circular orbit around a BH is evaluated by

$$R_{\text{ISCO}} = \frac{6GM_{\text{BH}}}{c^2} \gamma_{\pm}, \quad (6)$$

where  $c$  is the speed of light,  $\gamma_{\pm}$  represents the modification caused by the BH spin with respect to the disk on the location of the innermost stable circular orbit. It ranges from 1/6 for a maximally rotating BH surrounded by a prograde disk to 3/2 for a maximally rotating BH surrounded by a retrograde disk, assuming the disk and BH angular momenta are aligned (El Mellah 2017). For a non-rotating BH,  $\gamma_{\pm} = 1$ . Qin et al. (2018) found that the spin of the first formed BH in a binary is usually very low. For a considerable change of the spin, the BH needs to accrete an amount of mass of the order of its own mass (Wong et al. 2012). Regardless of the birth spin of the BH, we assume that the spin of the BH does not change during the BH+O phase as only a small fraction of the BH mass is accreted during this phase.

The specific angular momentum ( $j$ ) accreted by the BH from the O star wind can be written as (Shapiro & Lightman 1976, eq. 7)

$$j = \frac{1}{2} \eta \Omega_{\text{orb}} R_{\text{acc}}^2, \quad (7)$$

where  $\Omega_{\text{orb}}$  is the orbital angular velocity,  $\eta$  is a numerical factor which quantifies the efficiency of specific angular momentum accretion by the BH from the available wind matter and  $R_{\text{acc}}$  is the accretion radius which is the typical distance to the BH at which the wind trajectory and/or speed is significantly altered by the gravitational field of the BH. It can be written as (Davidson & Ostriker 1973)

$$R_{\text{acc}} = \frac{2GM_{\text{BH}}}{v_{\text{rel}}^2}, \quad (8)$$

where  $v_{\text{rel}} = \sqrt{v_{\text{wind}}^2 + v_{\text{orb}}^2}$  is the relative velocity of the stellar wind with respect to the BH for a circular orbit,  $v_{\text{wind}}$  is the wind velocity of the O star companion and  $v_{\text{orb}}$  is the relative velocity of the BH with respect to the O star, that is,  $v_{\text{orb}} = \Omega_{\text{orb}} a$ .

Eq. (7) was obtained under the assumption that the wind velocity is considerably larger than the orbital velocity, which is consistent with our further analysis (see Fig. B.1). If all wind material entering the accretion radius can be accreted by the BH,  $\eta = 1$  (Shapiro & Lightman 1976). Detailed hydrodynamical simulations suggest that this efficiency factor can be lower,  $\sim 1/3$  (Livio et al. 1986; Ruffert 1999). In what follows, we consider these two values.

Defining the mass ratio  $q = M_{\text{O}}/M_{\text{BH}}$  and combining Eqs. (5) - (8), the disk formation criterion can be converted into the dimensionless form

$$\frac{2}{3} \frac{\eta^2}{(1+q)^2} > \left( \frac{v_{\text{orb}}}{c} \right)^2 \left( 1 + \frac{v_{\text{wind}}^2}{v_{\text{orb}}^2} \right)^4 \gamma_{\pm}, \quad (9)$$

or equivalently

$$\frac{R_{\text{disk}}}{R_{\text{ISCO}}} = \frac{2}{3} \frac{\eta^2}{(1+q)^2} \left( \frac{v_{\text{orb}}}{c} \right)^{-2} \left( 1 + \frac{v_{\text{wind}}^2}{v_{\text{orb}}^2} \right)^{-4} \gamma_{\pm}^{-1} > 1. \quad (10)$$

Eqs. (9) and (10) suggest that a wind-captured disk can form around a BH if the captured material carries enough angular momentum, the wind speed is low compared to the orbital speed, and the orbital speed is high.

#### 2.4. X-ray luminosity

We can distinguish three cases for the morphology of the accretion flow: sub-Eddington accretion via a disk, super-Eddington accretion via a disk and spherical accretion. The first two happen only if enough angular momentum is carried by the accretion flow (see Sect. 2.3). Super-Eddington accretion occurs when the mass accretion rate is so high that the X-ray luminosity it produces exceeds the Eddington luminosity of the BH. Although super-Eddington accretion onto neutron stars has been observed in ultra-luminous X-ray sources (Bachetti et al. 2014; Fürst et al. 2016; Israel et al. 2017), the typical mass accretion rate calculated in our study is much smaller than the Eddington accretion rate for the individual systems (Fig. A.1). Accretion disks with a sub-Eddington mass accretion rate are thought to be geometrically thin and optically thick centrifugally-maintained structures (Shakura & Sunyaev 1973; Novikov & Thorne 1973). Notwithstanding minor relativistic corrections, such a disk around a BH radiates mostly in X-rays, and the maximum associated luminosity is (Frank et al. 2002; El Mellah 2017):

$$L_{\text{X}} = \frac{1}{2} \frac{GM_{\text{BH}} \dot{M}_{\text{acc}}}{R_{\text{ISCO}}}, \quad (11)$$

where  $\dot{M}_{\text{acc}}$  is the mass accretion rate.

In order to evaluate the mass accretion rate, we rely on the wind accretion formula introduced by Davidson & Ostriker (1973) (see also the review by Edgar 2004). It is valid in binary systems provided the wind speed at the binary orbital separation is larger than the orbital speed (El Mellah & Casse 2017). In this case, the fraction of the accreted wind can be approximated by

$$\frac{\dot{M}_{\text{acc}}}{\dot{M}_{\text{wind}}} = \frac{1}{4} \left( \frac{R_{\text{acc}}}{a} \right)^2 \frac{v_{\text{rel}}}{v_{\text{wind}}}, \quad (12)$$

where  $\dot{M}_{\text{wind}}$  is the O star wind mass loss rate.

Finally, in the case of spherical accretion, the mass accretion rate is not an independent variable. Instead, it is set by the location of the sonic point as described in the 1D spherical Bondi model (Bondi 1952). Without an accretion disk, thermal bremsstrahlung dominates the radiation from the optically thin wind material, which makes spherical accretion radiatively inefficient (Shapiro & Teukolsky 1983). We do not expect this regime to produce any X-ray emission above detectable levels.

#### 2.5. detectability of a BH+O system

The X-ray active lifetime ( $\tau_{\text{LX}}$ ) of each BH+O binary model considered is defined as the amount of time during the BH+O phase when the system is detectable as a wind-fed BH HMXB. We assume that this will be the case only when an accretion disk forms, that is, Eq. (10) is satisfied, and when the calculated X-ray luminosity (Eq. 11) and the distance to the source yield a flux above a detection threshold that we set to  $\sim 10^{-11}$  erg  $\text{s}^{-1}$

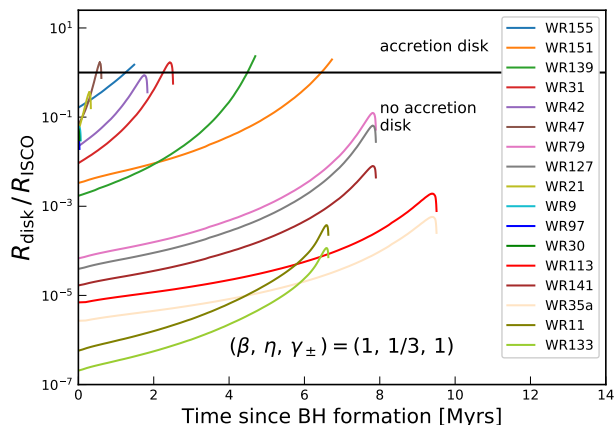


**Fig. 1.** Evolution of the ratio of circularisation radius  $R_{\text{disk}}$  to the radius of innermost stable circular orbit  $R_{\text{ISCO}}$  during the BH+O phase as a function of the time since the formation of the BH, for  $(\beta, \eta, \gamma_{\pm}) = (1, 1/3, 1)$ . The black horizontal line shows the dividing line above which an accretion disk is expected. The colour coding in the legend identifies the 17 progenitor WR+O star systems that are expected to give rise to the BH+O binaries.

$\text{cm}^{-2}$ . Our adopted threshold is similar to the flux detection limit of non-focussing X-ray telescopes with typical integration times (Wood et al. 1984; Bradt et al. 1991; In't Zand et al. 1994). We discuss the relevance of the X-ray flux threshold in the light of the sensitivity of current all-sky monitoring X-ray instruments in Sect. 5.

### 3. Results

#### 3.1. Fiducial parameter set

Figure 1 shows the evolution of the ratio of circularisation radius ( $R_{\text{disk}}$ ) to the radius of innermost stable circular orbit ( $R_{\text{ISCO}}$ ) during the BH+O phase, for the 17 progenitor WR+O star binaries. For our fiducial case, we adopt the value of  $\beta=1$  (Vink et al. 2001),  $\eta=1/3$  (El Mellah 2017) and  $\gamma_{\pm}=1$  (Qin et al. 2018). The O star expands during core hydrogen burning, leading to a decrease in its wind velocity, which makes the formation of a wind-captured disk easier during the late stages of its main sequence evolution. In most systems, there is a small decrease in the ratio of the circularisation radius to the innermost stable circular orbit towards the end of the BH+O star phase, which is related to the shrinkage of massive stars when they approach their core hydrogen depletion. WR139, WR151, and WR155 do not present this feature since their BH+O phases are terminated due to the Roche Lobe filling condition before their O stars complete core hydrogen burning. Whereas the mass ratio of WR 139 suggests this system will merge at this time, the other two could undergo an SS433-like evolution leading to short-period WR+BH binaries (van den Heuvel et al. 2017), which lies outside our present scope.

We find that no accretion disk forms in 12 of our BH+O models. Among them, three systems are not visible in this plot since the estimated rejuvenated age of their O stars are very close to the O stars' main sequence lifetime, such that the duration of their BH+O phase are very small. Importantly, we find that only in 5 BH+O models, all with orbital periods  $\leq 10$  days, an accretion disk can form for a small fraction of the total the BH+O

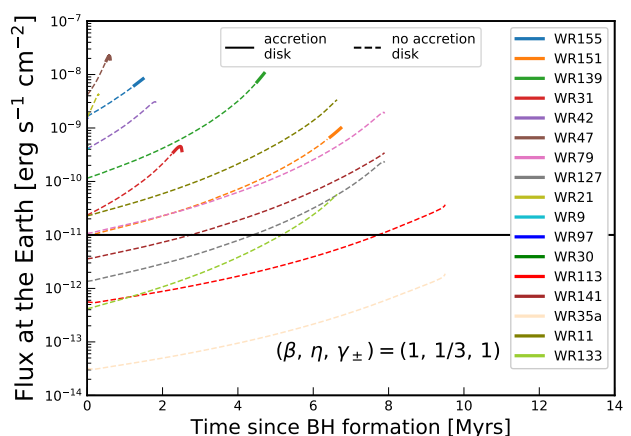
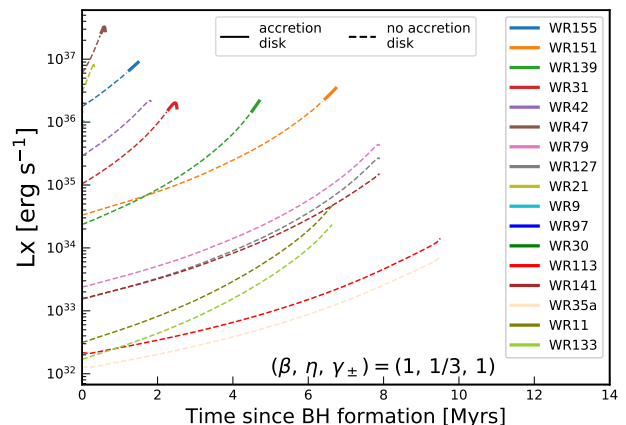


**Fig. 2.** Evolution of: X-ray luminosity (*upper panel*) calculated using Eq. (11), and the corresponding X-ray flux at Earth (*lower panel*) for our BH+O models when an accretion disk can form according to our criterion (solid line). The dashed lines indicate the X-ray luminosity and flux evolution if an accretion disk could form for the entire BH+O phase. The black horizontal line shows our adopted flux detection limit.

phase. For systems with higher orbital periods, an accretion disk does not form at all for the entire BH+O phase. Noting that the orbital period of WR 22 is  $\sim 80$  days, we do not expect that the BH+O binary anticipated to form from WR 22 will be X-ray bright at any time.

Figure 2 shows the X-ray luminosity (top panel) and its corresponding flux at Earth (bottom panel), calculated using Eq. (11) for our BH+O models. We find that when an accretion disk can form, the predicted X-ray flux at Earth is well above the flux detection limit we have assumed. In other words, the X-ray luminosity from the accretion disk is not a bottleneck for our BH+O models to be detectable in X-rays. We note that Eq. (11) only holds when an accretion disk is present such that the dashed lines are only indicative of the X-ray luminosity and flux if an accretion disk could form for the entire BH+O phase. The X-ray luminosity from a BH+O system without an accretion disk is expected to be orders of magnitude lower than what is predicted by Eq. (11) (see discussion in Sect. 2.4).

For each system where an accretion disk can form, we calculate the duration for which it will be detectable as a wind-fed BH HMXB (i.e. the X-ray active lifetime). To predict the number of wind-fed BH HMXB systems we expect based on

**Table 2.** Predicted X-ray active lifetime ( $\tau_{Lx}$ , in Myrs) of each of the 17 BH+O binary models and expected number of wind-fed black hole high mass X-ray binaries ( $N_{XRBs}$ , last line), for various combinations of  $\beta$ ,  $\eta$  and  $\gamma_{\pm}$ . The bold highlighted column represents our fiducial case.

$\gamma_{\pm}$	$(\beta, \eta)^a = (1, 1)$			$(\beta, \eta) = (0.8, 1)$			$(\beta, \eta) = (1, 1/3)$			$(\beta, \eta) = (0.8, 1/3)$		
	1/6	1	3/2	1/6	1	3/2	1/6	1	3/2	1/6	1	3/2
WR155	1.5	1.5	1.4	1.5	1.2	0.9	1.4	<b>0.2</b>	0.0	0.9	0.0	0.0
WR151	3.6	1.6	1.3	2.9	1.1	0.8	1.3	<b>0.3</b>	0.1	0.8	0.0	0.0
WR139	2.0	1.0	0.8	1.6	0.6	0.5	0.8	<b>0.2</b>	0.1	0.5	0.0	0.0
WR31	1.9	1.0	0.8	1.6	0.7	0.6	0.8	<b>0.2</b>	0.1	0.6	0.0	0.0
WR42	1.8	0.8	0.7	1.7	0.6	0.5	0.7	<b>0.0</b>	0.0	0.5	0.0	0.0
WR47	0.6	0.4	0.4	0.6	0.4	0.3	0.4	<b>0.1</b>	0.0	0.3	0.0	0.0
WR79	0.8	0.1	0.0	0.6	0.0	0.0	0.0	<b>0.0</b>	0.0	0.0	0.0	0.0
WR127	0.6	0.0	0.0	0.4	0.0	0.0	0.0	<b>0.0</b>	0.0	0.0	0.0	0.0
WR21	0.3	0.2	0.1	0.3	0.1	0.1	0.1	<b>0.0</b>	0.0	0.1	0.0	0.0
WR9	0.1	0.0	0.0	0.1	0.0	0.0	0.0	<b>0.0</b>	0.0	0.0	0.0	0.0
WR97	0.0	0.0	0.0	0.0	0.0	0.0	0.0	<b>0.0</b>	0.0	0.0	0.0	0.0
WR30	0.0	0.0	0.0	0.0	0.0	0.0	0.0	<b>0.0</b>	0.0	0.0	0.0	0.0
WR113	0.0	0.0	0.0	0.0	0.0	0.0	0.0	<b>0.0</b>	0.0	0.0	0.0	0.0
WR141	0.0	0.0	0.0	0.0	0.0	0.0	0.0	<b>0.0</b>	0.0	0.0	0.0	0.0
WR35a	0.0	0.0	0.0	0.0	0.0	0.0	0.0	<b>0.0</b>	0.0	0.0	0.0	0.0
WR11	0.0	0.0	0.0	0.0	0.0	0.0	0.0	<b>0.0</b>	0.0	0.0	0.0	0.0
WR133	0.0	0.0	0.0	0.0	0.0	0.0	0.0	<b>0.0</b>	0.0	0.0	0.0	0.0
$N_{XRBs}^b$	33.0	16.6	13.4	28.3	11.8	9.0	13.4	2.5	0.7	9.0	0.0	0.0

**Notes.** <sup>(a)</sup> see Eqs. (1) and (7) for the definition of  $\beta$  and  $\eta$  respectively. <sup>(b)</sup>  $N_{XRBs}$  is the predicted number of wind-fed BH high mass X-ray binaries by taking 0.4 Myrs as the typical lifetime of WR stars. See Sect. 3 for more details.

the 17 progenitor WR+O star systems, we assume (as in V20) that the observed numbers of WR+O binaries and wind-fed BH HMXBs are proportional to the lifetime in the respective phases. One WR+O binary is thus representative of  $\tau_{Lx}/\tau_{WR}$  wind-fed BH HMXBs, where  $\tau_{WR}$  is the duration of the WR+O binary phase. Taking  $\tau_{WR} = 0.4$  Myrs as the typical lifetime of a WR star (V20), we expect  $\sim 2.5$  wind-fed BH HMXBs from the 17 WR+O binaries. Accounting for the observational and theoretical bias in the population of WR+O binaries (see discussion in Sect. 2.1), it is likely that the number of wind-fed BH HMXBs in the entire Milky Way would be  $\sim 2$ -3.

### 3.2. Effects of parameter variations

The predicted number of wind-fed BH HMXBs is sensitive to the uncertainties in the parameters we have assumed. We explore the results computed using reasonable variations to our fiducial parameter set in Table 2. For a non-rotating BH ( $\gamma_{\pm}=1$ ), by varying  $(\beta, \eta)$  from (0.8, 1/6) to (1, 1/2), the predicted number of wind-fed BH HMXBs out of 17 WR+O binaries varies from 0 to 16.6. Considering a maximally spinning BH with a prograde accretion disk, the predicted number can be boosted up to 33, suggesting an observational bias in favour of wind-fed BH HMXBs containing maximally rotating BHs surrounded by a prograde disk. In the following subsections, we discuss the effects of these parameters individually.

#### 3.2.1. Efficiency of specific angular momentum accretion

From Eq. (10), the ratio of circularisation radius to the radius of the innermost stable orbit varies with the square of the efficiency of specific angular momentum accretion

$$\frac{R_{\text{disk}}}{R_{\text{ISCO}}} \propto \eta^2. \quad (13)$$

Article number, page 6 of 14

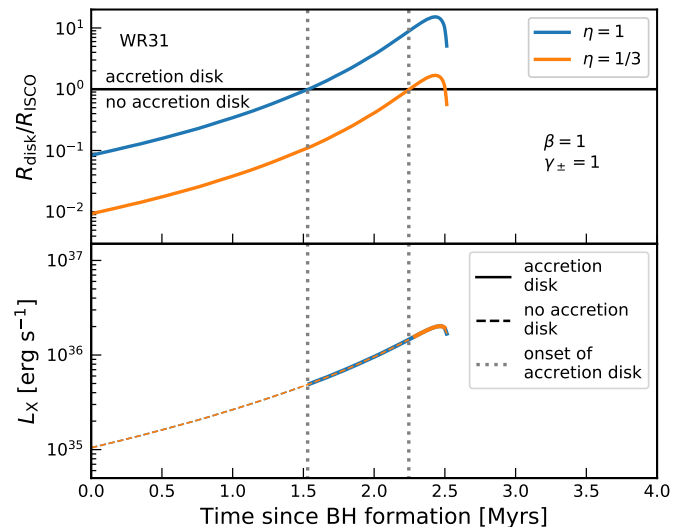


**Fig. 3.** Effects of  $\eta$  parameter on the ratio of the circularisation radius to the radius of the innermost stable circular orbit (upper panel) and the X-ray luminosity (lower panel). We take the BH+O binary derived from WR31 as an example. The  $\eta$  parameter is taken to be 1 and 1/3 (colour coded), and  $(\beta, \gamma_{\pm}) = (1, 1)$ . The line styles in the lower panel have the same meaning as in Fig. 2.

The predicted X-ray luminosity when an accretion disk can form does not depend on the efficiency parameter. So, the likelihood of the formation of an accretion disk in our BH+O models increases with the increase in the efficiency of angular momentum accretion by the BH. In Fig. 3, we show the variation of the above two quantities with the efficiency of specific angular momentum accretion, for the BH+O model corresponding to WR 31. We find that the amount of time an accretion disk can form during the BH+O phase is significantly longer when the efficiency of angu-

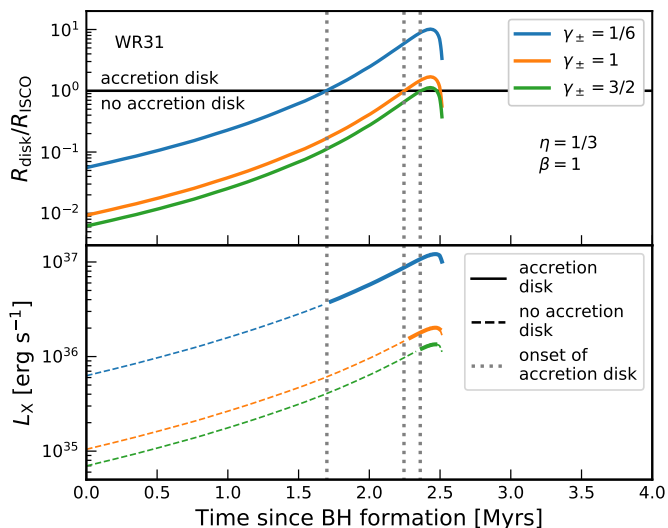


**Fig. 4.** Effects of the  $\gamma_{\pm}$  parameter. The same as Fig. 3 but  $\gamma_{\pm}$  is taken to be 1/6, 1, and 3/2 (colour coded), and  $(\beta, \eta) = (1, 1/3)$ . The line styles in the lower panel have the same meaning as in Fig. 2.

lar momentum accretion increases by a factor of 3. On the other hand, the X-ray luminosity predicted from Eq. (11) is unaffected. From Table 2, we find that the number of predicted wind-fed BH HMXBs increases by 6.5 times when the  $\eta$  increases from 1/3 to 1, and the other two parameters are at their fiducial value.

### 3.2.2. Black hole spin

Our definition of the radius of innermost stable circular orbit around a BH (Eq. 6) accounts for the effect of the spin of the BH on the formation of an accretion disk (via  $\gamma_{\pm}$ ). The spin parameter of BHs in observed wind-fed HMXBs can be quite high, as in Cyg X-1 (Gou et al. 2011; Zhao et al. 2021; Miller-Jones et al. 2021). To account for the spin of the BH, we calculate the predicted number of wind-fed BH HMXB derived from the 17 progenitor WR+O binaries for three cases (see Table 2): i) When the BHs are maximally rotating with a prograde accretion disk, ii) when the BHs are maximally rotating with a retrograde accretion disk, and iii) for a non-spinning BH.

Both the ratio of circularisation radius to the radius of the innermost stable orbit, and the X-ray luminosity from an accretion disk varies inversely with our BH spin parameter

$$\frac{R_{\text{disk}}}{R_{\text{ISCO}}} \propto \gamma_{\pm}^{-1} \quad (14)$$

and

$$L_X \propto \gamma_{\pm}^{-1}. \quad (15)$$

Figure 4 shows the effect of the BH spin on the formation of an accretion disk and the emitted X-ray luminosity during the BH+O phase of WR 31. For a BH maximally rotating with a prograde accretion disk, both the amount of time for which an accretion disk can form, and the X-ray luminosity predicted from the accretion disk increases significantly. In Table 2, we find that the predicted number of wind-fed HMXBs increases by a factor of  $\sim 5$  for the case of a maximally rotating BH with a prograde disk, and decreases by a factor of  $\sim 3.5$  for a maximally rotating BH with a retrograde disk, compared to a non-rotating BH, with the other two parameters are at their fiducial values.

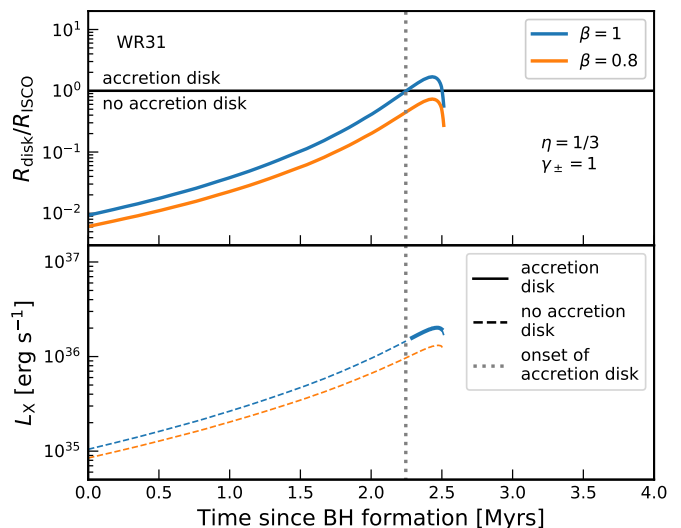


**Fig. 5.** Effects of the  $\beta$  parameter. The same as Fig. 3 but  $\beta$  parameter is taken to be 0.8 and 1 (colour coded), and  $(\eta, \gamma_{\pm}) = (1/3, 1)$ . The line styles in the lower panel have the same meaning as in Fig. 2.

The fact that we predict a short X-ray active lifetime for non-spinning BHs in BH+O systems, while the only observed wind-fed BH HMXB in the Milky Way is known to have high spin parameter, hints to the possibility that only BHs that were born with a very high spin are likely to be detectable as an X-ray source if they are associated with an O star in a close binary configuration. Qin et al. (2019) showed that high spin BHs can be produced only if the efficiency of angular momentum transport in stellar models is reduced. As such, BHs with high birth spins might be rare, as are observed wind-fed BH HMXBs.

### 3.2.3. O star wind velocity law

The exponent  $\beta$  in the wind velocity law for O stars is constrained from observations to be 0.8-1 (Groenewegen & Lamers 1989; Lamers et al. 1995; Puls et al. 1996). Since wind velocity is always larger than orbital velocity in our work, Eq. (10) and Eq. (11) suggest the dependencies

$$\frac{R_{\text{disk}}}{R_{\text{ISCO}}} \propto v_{\text{wind}}^{-8} \propto \left(1 - \frac{R_O}{a}\right)^{-8\beta}, \quad (16)$$

and

$$L_X \propto v_{\text{rel}}^{-3} \propto \left(1 - \frac{R_O}{a}\right)^{-3\beta}. \quad (17)$$

In our analysis, the ratio between the O star radius (obtained from the stellar tracks of Ekström et al. 2012) and orbital separation is generally below 0.4. Therefore, changing  $\beta$  from 1 to 0.8 can maximally reduce the ratio of the circularisation radius to the radius of the innermost stable circular orbit by a factor of  $\sim 2$ , making the formation of accretion disk more difficult. Likewise, the predicted X-ray luminosity from Eq. (11) is also decreased.

We present the effects of the  $\beta$  parameter on the formation of an accretion disk and the X-ray luminosity emitted from the disk in Fig. 5, where we take the BH+O model derived from WR 31 as an example. We find that even the change in the assumed  $\beta$  value from 1 to 0.8 makes the BH+O model of WR 31 to become X-ray inactive due to the inability to form an accretion disk. The

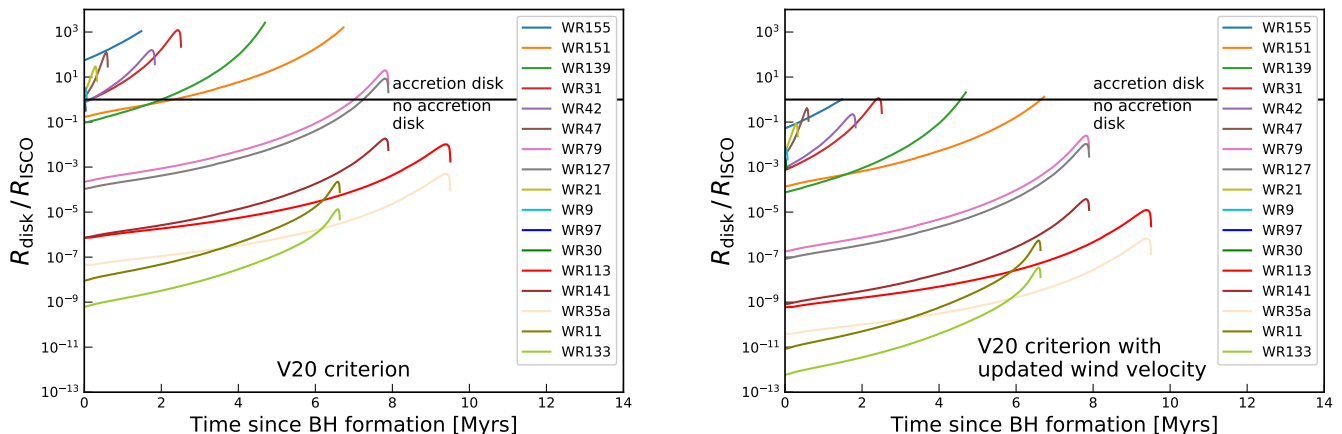


**Fig. 6.** Evolution of the ratio of circularisation radius of the accreted wind matter from the O star to the radius of innermost stable circular orbit of the BH for the 17 BH+O star binary models as a function of the time since the formation of the BH. The left panel shows the evolution as calculated by V20, that does not account for the orbital velocity of the companion and the typical wind velocity of O stars. The right panel shows the same evolution when we use the typical O star wind velocity (Eq. 1), the mass of the BH, and the orbital velocity of the O star companion. The black horizontal line in both the panels show the dividing line above which an accretion disk can form. The colour coding in the legend identifies the 17 progenitor WR+O star systems that are expected to give rise to the BH+O binaries.

predicted X-ray luminosity and thereby the X-ray flux from an accretion disk, if it were to form, is also decreased, but not as significantly as to fall beyond our flux detection limit.

From Table 2, we see that when we change the value of the  $\beta$  from 1 to 0.8 (other parameters remaining at their fiducial values), our BH+O binary models do not have any X-ray bright phase. The predicted number of wind-fed BH HMXBs decreases from  $\sim 2.5$  to zero. This shows that the X-Ray active lifetime of the BH+O binaries analysed in our work is very sensitive to the assumed wind velocity of the O star companion.

#### 4. Comparison with earlier work

Starting from the same 17 WR+O binaries, V20 performed a similar analysis and predicted to find over 200 wind-fed BH HMXBs in the Milky Way. Here, we compare the analysis of V20 with our work and discuss the factors that lead to the difference in the predicted numbers.

V20 adopted the accretion disk formation criterion derived by Iben & Tutukov (1996). Iben & Tutukov (1996) primarily modelled accretion onto degenerate white dwarfs from red giant donors and their central idea remained the same in the sense that they assumed that an accretion disk forms when the specific angular momentum of the accreted matter exceeds that of the innermost stable circular orbit radius of the BH. Iben & Tutukov (1996) assumed that the specific angular momentum ( $j$ ) accreted by the degenerate dwarf from the stellar wind of the giant companion is given by

$$j \sim \Omega_g R_g^2 \left( \frac{R_{\text{acc}}}{a} \right)^2, \quad (18)$$

where  $\Omega_g$  and  $R_g$  are the angular velocity and radius of the giant star respectively. Iben & Tutukov (1996) defined the accretion radius  $R_{\text{acc}}$  as

$$R_{\text{acc}} = \frac{2GM_{\text{dd}}}{v_{\text{wind}}^2}, \quad (19)$$

where  $M_{\text{dd}}$  is the mass of the degenerate dwarf. They further assumed that the companion star is tidally locked and the binary mass is dominated by the giant star mass ( $M_g$ ). Comparing our work and V20, we note the difference of a factor  $\sim R_g^2/a^2$  in the definition of specific angular momentum accretion, and the omission of the relative velocity of the BH with respect to the main sequence companion in the definition of the accretion radius. For the wind velocity, Iben & Tutukov (1996) assume that the wind velocity from the giant companions is given by

$$v'_{\text{wind}} = v'_{\text{esc}} \left( 1 - \frac{R_g}{a} \right), \quad (20)$$

where  $v'_{\text{esc}} = \sqrt{2GM_g/R_g}$  is the escape velocity from the companion star. Effectively, they assumed that the terminal wind velocity is equal to the escape velocity from the surface of the star, and  $\beta=1$ . They also did not take into account the Eddington factor.

Observational studies of the terminal wind velocities of O stars show that their terminal velocities are larger than their escape velocities, such that the appropriate expression for the wind velocity from O stars is given by Eq. (1) (Vink et al. 2001). However, V20 did not account for the typical wind velocity of the O stars when they adopted the disk formation criterion derived by Iben & Tutukov (1996) for their BH+O systems, that is, the terminal wind velocities used by V20 in their disk formation criterion are underestimated by a factor of 2.6.

Figure 6 shows the evolution of the ratio of circularisation radius to the radius of innermost stable circular orbit during the BH+O phase of the 17 progenitor WR+O binaries, with (*right panel*, Eq. C.1) and without (*left panel*, Eq. C.3) taking into consideration the typical O star wind velocity, the mass of the O star, and the orbital velocity in the definition of accretion radius. Comparing the left and right hand side panels, we see that using the appropriate O star wind velocity, the fraction of the BH+O star phase when an accretion disk can form greatly decreases. This shows that the X-ray active lifetime is very sensitive to the wind velocity considered in the disk formation criterion.

From the modified criterion (Eq. C.1), we see that only 4 out of 17 progenitor WR+O binaries are to become wind-fed BH

HMXBs for a short period during their lifetime as a BH+O star binary. All of them are close binaries with orbital periods less than 10 days. The only observed wind-fed BH+O in the Milky Way, Cyg X-1, also has an orbital period of around  $\sim 5.6$  days (Orosz et al. 2011; Hirsch et al. 2019). From the modified criterion, we expect to find  $\sim 3$  wind-fed BH HMXBs for the 17 progenitor WR+O binaries instead of 44 as calculated in V20.

In the definition of the accretion radius (Eq. 19), Iben & Tutukov (1996) only account for the wind velocity of the giant star companion and not for the relative velocity between the compact object and the red giant star. We find that this assumption does not play a significant role in most of our BH+O systems as the wind velocity is much larger than the orbital velocity (Fig. B.1). But for systems where the wind velocity can be comparable to the orbital velocity, the inclusion of the orbital velocity can further reduce the X-ray active lifetime.

Iben & Tutukov (1996) also approximated the total mass of the binary system to be approximately equal to the mass of the giant star companion (see their eq. 65). Their work was primarily aimed at white dwarf/neutron star+red giant binary systems and hence this was a reasonable approximation. However, that approximation breaks down for BH+O systems. V20 did not correct for the mass of the BH in the equation of the orbital velocity. The inclusion of the mass of the BH in the expression for orbital velocity reduces the predicted X-ray active lifetime of the BH+O models for systems where the mass of the BH formed is comparable to the mass of the O star, most readily seen from Eq. (C.2). For an equal mass BH+O binary, accounting for the mass of the BH introduces a factor of  $\sim 1.34$  in the right hand side of Eq. (C.2), which means that the radius of the O star has to be larger, all other parameters fixed, for an accretion disk to form.

The luminosity of massive O stars can be a finite fraction of its Eddington luminosity (see Table 1). Accounting for this Eddington factor, defined as the ratio of the luminosity of the O star to its Eddington luminosity, in the wind velocity of O stars leads to a decrease in the calculated O star wind velocity. However, in many of our considered WR+O binaries, the Eddington factor of the O star is low ( $\leq 0.1$ ). Hence, the inclusion of the Eddington factor does not have a significant effect on the predicted X-ray active lifetime of most of our BH+O models. On the other hand, for the few systems which have Eddington factors  $\sim 0.3$ , accounting for the Eddington factor increased the X-ray active lifetime, but not as significantly as to compensate for the updated O star terminal wind velocity.

For the X-ray emission from a BH+O model with an accretion disk to be detectable from Earth, V20 assumed a luminosity cut-off of  $10^{35}$  erg  $s^{-1}$  for all the 17 systems regardless of their individual distances from Earth. But most of the 17 WR+O binaries considered are not located within 3-4 kpc. In our work, we assume a flux cut-off of  $\sim 10^{-11}$  erg  $s^{-1}$   $cm^{-2}$ , and take the distance of each source from Earth into consideration individually. The consideration of the individual distances does not affect our results as the calculated X-ray flux is above our flux detection threshold for all the models that are predicted to have an X-ray active phase (Fig. 2).

The end of the BH+O phase in V20 is taken to be the point when the companion star fills its Roche lobe. This can lead to an over-prediction of  $\tau_{Lx}$  for comparatively wide systems where the O star can complete hydrogen burning and yet not fill its Roche lobe. Since the wind velocity of post MS stars are low as well, some of these systems in the post MS phase of the O star can become strong X-ray emitters but do not necessarily fall under the class of wind-fed BH HMXBs. Hence, V20 may have over-

predicted the X-ray active lifetime for some of the progenitor WR systems binaries by including the post-MS phase.

A recent population synthesis study by Shao & Li (2020) based on rapid binary evolution code predicted about 10 - 30 wind-fed BH HMXBs in the Milky Way (see also, Wiktorowicz et al. 2020). The mass loss rate in Vink et al. (2001) is adopted, and the accretion rate is evaluated by the Bondi-Hoyle-Lyttleton accretion model (Bondi & Hoyle 1944; Belczynski et al. 2008). To evaluate the detectability of their BH+O binary models, they also adopt the same threshold for X-ray luminosity at  $10^{35}$  erg/s as V20. We note that they did not take into account the criterion for the formation of an accretion disk. Our work suggests that accretion disks can only exist for a limited period of the main sequence lifetime of the O stars, which mainly determines the X-ray active lifetime of the BH+O star binaries. Therefore, Shao & Li (2020) have likely overestimated the number of wind-fed BH HMXBs in the Milky Way.

## 5. Discussion

Here, we discuss the uncertainties in the predicted X-ray active lifetimes of our BH+O binary models.

### 5.1. Specific angular momentum accretion

The discrepancy between the predicted wind-fed BH HMXB populations of V20 and our work shows that the criterion for accretion disk formation is sensitive to variations of the parameters in the theory. In particular, accounting for a larger O star wind velocity changes the prediction of V20 drastically. More factors such as the accretion efficiency, and the approximation of the specific angular momentum carried by the accreted matter introduce further uncertainties for the computation of the X-Ray bright lifetime of the BH+O star binaries (Sect. 3). Livio et al. (1986) and Soker et al. (1986) studied accretion onto compact objects using detailed hydrodynamic simulations and found that while the mass accretion rate is similar to that predicted by the Bondi-Hoyle theory, the amount of specific angular momentum accreted was only a few percent of that predicted by the analytical approximation obtained from the Bondi-Hoyle theory. A similar conclusion was drawn by Ruffert (1999).

Owing to these calculations, El Mellah (2017) adopted the analytical expression for specific angular momentum from Shapiro & Lightman (1976, eq. 7) but introduced an efficiency factor of 1/3 to account for the reduced specific angular momentum accretion found in the detailed numerical hydrodynamic studies. We captured this uncertainty and studied its effects through our efficiency parameter  $\eta$ . Therefore, we need to compare the analytical approximations to the specific angular momentum carried by the accreted matter used in V20 and our work, to detailed 3D numerical hydrodynamic simulations to assess the reliability of the approximations.

As a preliminary exercise, in Fig. 7, we compare the expression for specific angular momentum carried by the wind matter used in V20 (eq. 62 of Iben & Tutukov 1996) to the analytical form derived by Shapiro & Lightman (1976) that is assumed in our work. We see that there are significant differences between the two definitions, and to the third, which includes the typical O star wind velocity in expression for specific angular momentum carried by the wind matter given by Iben & Tutukov (1996).

Due to the line-deshadowing instability and sub-photospheric turbulence, stellar winds from hot stars are prone to form overdense regions called ‘‘clumps’’ (Owocki &

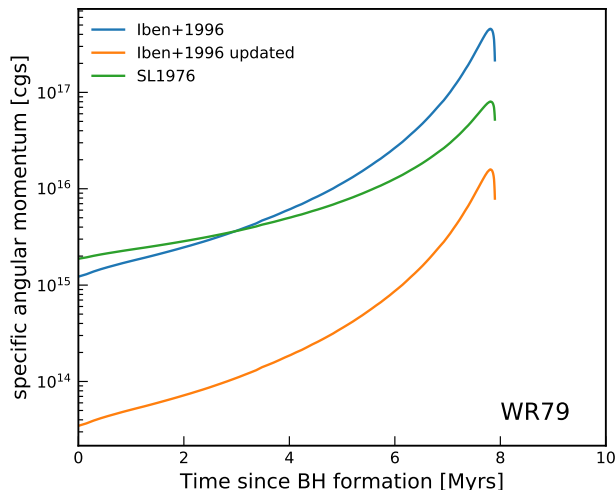


**Fig. 7.** Comparison of the specific angular momentum of the accreted wind matter used in V20 (Eq. 18, Iben+1996), to the analytical value derived by Shapiro & Lightman (1976) (SL1976), for the stellar and binary parameters of WR79, as a function of the time since black hole formation. We also show the decrease in the amount of specific angular momentum carried by the wind when the typical wind velocity for O type stars is introduced in Eq. (18), denoted by ‘Iben+1996 updated’.

Rybicki 1984; Owocki et al. 1988; Feldmeier 1995; Grassitelli et al. 2015). These clumps produce stochastic variations in the instantaneous amount of specific angular momentum of the accreted material. These variations take place on time scales of the order of hundreds to thousands of seconds, much shorter than the evolutionary time scales (Grinberg et al. 2017; El Mellah et al. 2020b). For clump sizes derived from first principles (Sundqvist et al. 2018), clumps are small compared to the accretion radius when they reach the orbital separation (El Mellah et al. 2018). As a consequence, they induce a limited peak-to-peak variability. However, when the wind is sufficiently fast, the net amount of angular momentum provided to the flow is so small (and so is the accretion radius) that the serendipitous capture of clumps becomes relatively more important and can produce a transient accretion disk. However, in Cygnus X-1, the wind-captured disk is permanent and so far, the only wind-fed HMXB where a transient wind-captured disk was observed is Vela X-1 (Liao et al. 2020). In the latter case, the disk formation is believed to be associated to variations at the periastron induced by the slightly eccentric orbital motion, rather than to clump capture (Kretschmar et al. 2021). Therefore, including wind clumping is not expected to significantly modify the results obtained in this paper.

## 5.2. Properties of the WR star companion

In many of the investigated WR+O star binaries, in particular in the shorter-period ones, the WR star likely formed via Roche-lobe overflow from its progenitor O star (e.g. Vanbeveren et al. 1998a; Wellstein & Langer 1999). The companion O star may thus accrete mass from the WR star progenitor, which could lead to properties which are different from those of single O stars. Important properties in this respect are the helium abundance and spin of the mass gaining O star.

An enhancement of the surface helium mass fraction of the mass gainer of a few percent is predicted from conservative (Wellstein & Langer 1999) as well as non-conservative (Petrovic et al. 2005a; Langer et al. 2020) massive binary evolution models. This enrichment leads to a slight overluminosity of the mass gainer (Langer 1992), which may affect the stellar wind properties. However, quantitatively, this effect is not expected to exceed the uncertainty in the average wind properties of O stars (Vink & Sander 2021).

Independent of the mass transfer efficiency, the angular momentum gain of the accretor during the mass transfer is expected to spin-up the mass gainer significantly (Packet 1981; Petrovic et al. 2005b; Langer et al. 2020). The observed population of Be/X-ray binaries (Reig 2011) signifies that this spin-up may achieve near-critical rotation, with strong consequences for the mass outflow from the spun-up star, and the mass accretion onto the compact companion. The Galactic and LMC WR+O binaries indeed also contain rapidly rotating O stars (Vanbeveren et al. 2018; Shara et al. 2020). However, while faster than average O stars, the analysed WR companions rotate on average with less than 50% of their critical rotational velocity, implying that the centrifugal force remains below 25% of the surface gravity at the stellar equator. Whereas this may lead to a slight wind anisotropy, a disk-like outflow is not expected in this case.

In our analysis above, we adopted a wind velocity of the O star companions as expected for single stars. However, in Be/X-ray binaries (Waters et al. 1988) as well as in supergiant X-ray binaries (Manousakis et al. 2012), abnormally slow stellar winds are observed. While in the first case, this may relate to the stars’ extreme rotation, a reduced wind acceleration due to the X-ray irradiation of the stellar atmosphere is thought to be responsible in the latter case (see also, Vilhu et al. 2021). For the conclusions we draw above, the consequences would be small, since none of the two effects is expected in the majority of the investigated binaries. For the few cases where disk formation and significant X-ray emission is predicted, a slower wind would, however, lead to an increased accretion rate and a higher X-ray luminosity.

## 5.3. Other uncertainties

The lifetime of WR+O star binary phase is taken to be constant for all the different considered WR+O binaries, whereas it actually depends on the core helium burning lifetime of the WR star, which in turn depends on the individual masses of the WR star. However, we do not expect this simplifying assumption to affect our predicted number of wind-fed BH HMXBs significantly. The mass of the WR stars at the end of core helium depletion is also uncertain due to the uncertainty in the mass loss rate during the WR phase (Neijssel et al. 2021). In both works, ours and V20, it is assumed that the properties of the WR stars do not change after core helium depletion. However, it has been shown recently (Laplace et al. 2020) that WR stars that have an outer hydrogen envelope may expand post helium depletion and the binary can undergo another mass transfer phase before core collapse (see also Laplace et al. 2021). Therefore, the formation of wind-fed BH HMXBs needs further investigation, both using detailed binary evolution models that calculate the binary evolution up to the core collapse of the WR star as well as into accurate modelling of the physics of accretion onto BHs.

We have shown (Fig. A.1) that the predicted mass accretion rates calculated for the anticipated BH+O binaries are much lower than the Eddington mass accretion rates. Hence, we don’t consider super-Eddington accretion to be relevant to our work. Due to the same reason, the X-ray emission should be isotropic

and we do not need to consider the case of beaming (King 2008). LOBSTER eye telescopes can reach a flux cut-off of  $10^{-12}$  erg  $s^{-1}$   $cm^{-2}$  (Priedhorsky et al. 1996; Hudec et al. 2007). The recently launched eROSITA X-ray telescope is stated to have a flux detection threshold of  $\sim 10^{-14}$  erg  $s^{-1}$   $cm^{-2}$  (Merloni et al. 2012) in the average all-sky survey mode. However, changing the flux limit to these lower values does not change our predicted X-ray active lifetime as once a wind-captured disk can form around the BH, the expected X-ray flux at Earth is higher than  $10^{-11}$  erg  $s^{-1}$   $cm^{-2}$  (Fig. 2). On the other hand, if there is significant extinction at X-ray wavelengths in the Galactic plane, our predicted X-ray active lifetime of the BH+O binary models can get reduced.

The predicted X-ray luminosity of an accreting BH in our models is a few percent of the Eddington luminosity. In such a case, the X-ray spectrum can switch from a soft state to a hard state and the X-ray emission becomes radiatively inefficient (Yuan & Narayan 2014). This is well-described by a distended and tenuous advection-dominated accretion flow (ADAF, see Narayan & Yi 1994, 1995a,b). In this accretion regime, the bulk of the accretion energy is carried by the accreting gas in the form of thermal energy, that can vanish through the event horizon of the BH. Hence, the black holes in the ADAF regime can be fainter by a factor of  $\sim 100$ -1000 (Narayan & McClintock 2008). In such a case, we do not expect the binary to be detectable in X-rays. Inclusion of this effect can only reduce our prediction of the X-ray active lifetime during the BH+O phase.

## 6. Conclusion

WR+O binaries are expected to be progenitors of BH+O binaries. V20 investigated 17 galactic WR+O star binaries and predicted that there should be more than 200 wind-fed BH HMXBs in the Milky Way while only one has been observed. They concluded that BHs receive much higher natal kick velocities or WR stars explode with supernova explosions to form neutron stars, which lead to a break-up of the binary systems.

We apply a similar methodology as in V20 with an improved analytical criterion to study the formation of accretion disks around BHs in BH+O binaries and the detectability of X-ray emission from such systems. We also investigate the effect of uncertain physics parameters, such as the  $\beta$  value in the O star wind velocity law, the efficiency of angular momentum accretion ( $\eta$ ) and the spin of the BH ( $\gamma_{\pm}$ ), on the predicted number of wind-fed BH HMXBs. We find that this calculated number is sensitive to plausible variations of the assumed parameters.

For our fiducial parameter set  $(\beta, \eta, \gamma) = (1, 1/3, 1)$  (see Sect. 3, and Fig. 1), we predict only  $\sim 2$ -3 wind-fed BH HMXBs based on the 17 progenitor WR+O systems. While we still over-predict the number of wind-fed BH HMXBs, accounting for the theoretical and observational biases in the population of WR+O binaries (see Sect. 2.1) suggest that we should expect  $\sim 2$ -3 wind-fed BH HMXBs in the entire Milky Way. We remind the reader that only 1 wind-fed BH+O X-ray binary has been observed (Cyg X-1).

We then revisited the derivation of the accretion disk formation criterion used by V20 and found that, in particular, the assumed O star wind velocity was underestimated. Accounting for the appropriate O star wind velocity (Vink et al. 2001), we find most of BH+O binary models will have negligible X-ray bright lifetimes due to the absence of an accretion disk around the BH (see Fig. 6). As such, any conclusion drawn from the seemingly discrepant number of observed WR+O binaries and wind-fed BH HMXBs has to be re-evaluated.

Our analysis shows further that a high BH spin parameter can lead to significantly longer and brighter X-ray phases in wind-accreting BH+O binaries. The corresponding bias in detecting such binaries with rapidly spinning BHs may help to alleviate the tension between the rather low BH spin values generally predicted from binary stellar evolution models (Qin et al. 2018), and the high BH spin values observationally deduced from BH+O binaries in the Local Group (Qin et al. 2019).

We conclude that high BH formation kicks are not necessary to understand the number discrepancy between the populations of observed WR+O binaries and wind-fed BH HMXBs in the Milky Way. With our current understanding of O star wind velocities, we have shown that possibly the vast majority of Galactic BH+O star binaries may not form BH accretion disks and hence remain undetected in X-Ray surveys. Recent studies have shown that the GAIA satellite offers an excellent opportunity to observe X-ray such quiet BH+O binaries via periodic astrometric variations (Breivik et al. 2017; Mashian & Loeb 2017; Yalinewich et al. 2018; Yamaguchi et al. 2018; Andrews et al. 2019). Furthermore, BH+O binaries can also be detected from photometric variability of the O star induced by the BH companion (Zucker et al. 2007; Masuda & Hotokezaka 2019), or spectroscopically via the periodic shift in radial velocity of the O star.

*Acknowledgements.* We thank Pablo Marchant and Krzysztof Belczynski for meaningful discussions, and Dany Vanbeveren for helpful comments on an earlier version of this manuscript. I.E.M. has received funding from the European Research Council (ERC) under the European Union's Horizon 2020 research and innovation programme (Spawn ERC, grant agreement No 863412). This research has made use of NASA's Astrophysics Data System.

## References

- Abbott, B. P., Abbott, R., Abbott, T. D., et al. 2016, *Physical Review X*, 6, 041015
- Abbott, B. P., Abbott, R., Abbott, T. D., et al. 2019, *Physical Review X*, 9, 031040
- Andrews, J. J., Breivik, K., & Chatterjee, S. 2019, *ApJ*, 886, 68
- Bachetti, M., Harrison, F. A., Walton, D. J., et al. 2014, *Nature*, 514, 202
- Balbus, S. A. & Hawley, J. F. 1991, *ApJ*, 376, 214
- Belczynski, K., Buonanno, A., Cantiello, M., et al. 2014, *ApJ*, 789, 120
- Belczynski, K., Kalogera, V., Rasio, F. A., et al. 2008, *The Astrophysical Journal Supplement Series*, 174, 223
- Belczynski, K., Klencki, J., Fields, C. E., et al. 2020, *A&A*, 636, A104
- Belczynski, K., Repetto, S., Holz, D. E., et al. 2016, *ApJ*, 819, 108
- Belczynski, K., Wiktorowicz, G., Fryer, C. L., Holz, D. E., & Kalogera, V. 2012, *ApJ*, 757, 91
- Bondi, H. 1952, *MNRAS*, 112, 195
- Bondi, H. & Hoyle, F. 1944, *MNRAS*, 104, 273
- Bradt, H. V., Swank, J. H., & Rothschild, R. E. 1991, *Advances in Space Research*, 11, 243
- Brandt, W. N., Podsiadlowski, P., & Sigurdsson, S. 1995, *MNRAS*, 277, L35
- Braun, H. & Langer, N. 1995, *A&A*, 297, 483
- Breivik, K., Chatterjee, S., & Larson, S. L. 2017, *ApJ*, 850, L13
- Crowther, P. A. 2015, in *Wolf-Rayet Stars*, ed. W.-R. Hamann, A. Sander, & H. Todt, 21–26
- Crowther, P. A. 2019, *Galaxies*, 7, 88
- Davidson, K. & Ostriker, J. P. 1973, *ApJ*, 179, 585
- de Mink, S. E. & Belczynski, K. 2015, *ApJ*, 814, 58
- de Mink, S. E. & Mandel, I. 2016, *MNRAS*, 460, 3545
- Dhawan, V., Mirabel, I. F., Ribó, M., & Rodrigues, I. 2007, *ApJ*, 668, 430
- du Buisson, L., Marchant, P., Podsiadlowski, P., et al. 2020, *MNRAS*, 499, 5941
- Edgar, R. 2004, *New A Rev.*, 48, 843
- Ekström, S., Georgy, C., Eggenberger, P., et al. 2012, *A&A*, 537, A146
- El Mellah, I. 2017, arXiv e-prints, arXiv:1707.09165
- El Mellah, I., Bolte, J., Decin, L., Homan, W., & Keppens, R. 2020a, *A&A*, 637, A91
- El Mellah, I. & Casse, F. 2017, *MNRAS*, 467, 2585
- El Mellah, I., Grinberg, V., Sundqvist, J. O., Driessen, F. A., & Leutenegger, M. A. 2020b, *A&A*, 643, A9
- El Mellah, I., Sundqvist, J. O., & Keppens, R. 2018, *MNRAS*, 475, 3240

- Event Horizon Telescope Collaboration, Akiyama, K., Alberdi, A., et al. 2019, *ApJ*, 875, L1
- Farr, W. M., Sravan, N., Cantrell, A., et al. 2011, *ApJ*, 741, 103
- Feldmeier, A. 1995, *A&A*, 299, 523
- Fragos, T., Willems, B., Kalogera, V., et al. 2009, *ApJ*, 697, 1057
- Frank, J., King, A., & Raine, D. J. 2002, *Accretion Power in Astrophysics: Third Edition*
- Fujita, Y., Inoue, S., Nakamura, T., Manmoto, T., & Nakamura, K. E. 1998, *ApJ*, 495, L85
- Fürst, F., Walton, D. J., Harrison, F. A., et al. 2016, *ApJ*, 831, L14
- Gou, L., McClintock, J. E., Reid, M. J., et al. 2011, *ApJ*, 742, 85
- Grassitelli, L., Fossati, L., Simón-Díaz, S., et al. 2015, *ApJ*, 808, L31
- Grinberg, V., Hell, N., El Mellah, I., et al. 2017, *A&A*, 608, A143
- Groenewegen, M. A. T. & Lamers, H. J. G. L. M. 1989, *A&AS*, 79, 359
- Hirsch, M., Hell, N., Grinberg, V., et al. 2019, *A&A*, 626, A64
- Hobbs, G., Lorimer, D. R., Lyne, A. G., & Kramer, M. 2005, *MNRAS*, 360, 974
- Hudec, R., Pina, L., Šimon, V., et al. 2007, *Nuclear Physics B Proceedings Supplements*, 166, 229
- Iben, Icko, J. & Tutukov, A. V. 1996, *ApJS*, 105, 145
- Illarionov, A. F. & Sunyaev, R. A. 1975, *A&A*, 39, 185
- In't Zand, J. J., Priedhorsky, W. C., Moss, C. E., et al. 1994, in *Society of Photo-Optical Instrumentation Engineers (SPIE) Conference Series*, Vol. 2279, *Advances in Multilayer and Grazing Incidence X-Ray/EUV/FUV Optics*, ed. R. B. Hoover & A. B. Walker, 458–468
- Israel, G. L., Belfiore, A., Stella, L., et al. 2017, *Science*, 355, 817
- King, A. R. 2008, *MNRAS*, 385, L113
- Kremer, K., Lu, W., Rodriguez, C. L., Lachat, M., & Rasio, F. A. 2019, *ApJ*, 881, 75
- Kretschmar, P., El Mellah, I., Martínez-Núñez, S., et al. 2021, *arXiv e-prints*, arXiv:2104.13148
- Kruckow, M. U., Tauris, T. M., Langer, N., Kramer, M., & Izzard, R. G. 2018, *MNRAS*, 481, 1908
- Lamers, H. J. G. L. M., Snow, T. P., & Lindholm, D. M. 1995, *ApJ*, 455, 269
- Langer, N. 1992, *A&A*, 265, L17
- Langer, N. 2012, *ARA&A*, 50, 107
- Langer, N., Schürmann, C., Stoll, K., et al. 2020, *A&A*, 638, A39
- Laplace, E., Göteborg, Y., de Mink, S. E., Justham, S., & Farmer, R. 2020, *A&A*, 637, A6
- Laplace, E., Justham, S., Renzo, M., et al. 2021, *arXiv e-prints*, arXiv:2102.05036
- Liao, Z., Liu, J., Zheng, X., & Gou, L. 2020, *MNRAS*, 492, 5922
- Livio, M., Soker, N., de Kool, M., & Savonije, G. J. 1986, *MNRAS*, 222, 235
- Mandel, I. & Müller, B. 2020, *MNRAS*, 499, 3214
- Mandel, I., Müller, B., Riley, J., et al. 2021, *MNRAS*, 500, 1380
- Manousakis, A., Walter, R., & Blondin, J. M. 2012, *A&A*, 547, A20
- Marchant, P., Langer, N., Podsiadlowski, P., Tauris, T. M., & Moriya, T. J. 2016, *A&A*, 588, A50
- Mashian, N. & Loeb, A. 2017, *MNRAS*, 470, 2611
- Masuda, K. & Hotokezaka, K. 2019, *ApJ*, 883, 169
- Mennekens, N. & Vanbeveren, D. 2014, *A&A*, 564, A134
- Merloni, A., Predehl, P., Becker, W., et al. 2012, *arXiv e-prints*, arXiv:1209.3114
- Miller-Jones, J. C. A., Bahramian, A., Orosz, J. A., et al. 2021, *Science*, 371, 1046
- Minniti, D., Contreras Ramos, R., Alonso-García, J., et al. 2015, *ApJ*, 810, L20
- Mirabel, I. F. & Rodríguez, I. 2003, *Science*, 300, 1119
- Narayan, R. & McClintock, J. E. 2008, *New A Rev.*, 51, 733
- Narayan, R. & Yi, I. 1994, *ApJ*, 428, L13
- Narayan, R. & Yi, I. 1995a, *ApJ*, 444, 231
- Narayan, R. & Yi, I. 1995b, *ApJ*, 452, 710
- Neijssel, C. J., Vinciguerra, S., Vigna-Gómez, A., et al. 2021, *ApJ*, 908, 118
- Novikov, I. D. & Thorne, K. S. 1973, in *Black Holes (Les Astres Occlus)*, 343–450
- O'Connor, E. & Ott, C. D. 2011, *ApJ*, 730, 70
- Orosz, J. A., McClintock, J. E., Aufdenberg, J. P., et al. 2011, *ApJ*, 742, 84
- O'Shaughnessy, R., Kim, C., Kalogera, V., & Belczynski, K. 2008, *ApJ*, 672, 479
- Owocki, S. P., Castor, J. I., & Rybicki, G. B. 1988, *ApJ*, 335, 914
- Owocki, S. P. & Rybicki, G. B. 1984, *ApJ*, 284, 337
- Özel, F., Psaltis, D., Narayan, R., & McClintock, J. E. 2010, *ApJ*, 725, 1918
- Packet, W. 1981, *A&A*, 102, 17
- Perets, H. B., Li, Z., Lombardi, James C., J., & Milcarek, Stephen R., J. 2016, *ApJ*, 823, 113
- Petrovic, J., Langer, N., & van der Hucht, K. A. 2005a, *A&A*, 435, 1013
- Petrovic, J., Langer, N., Yoon, S. C., & Heger, A. 2005b, *A&A*, 435, 247
- Priedhorsky, W. C., Peele, A. G., & Nugent, K. A. 1996, *MNRAS*, 279, 733
- Puls, J., Kudritzki, R. P., Herrero, A., et al. 1996, *A&A*, 305, 171
- Qin, Y., Fragos, T., Meynet, G., et al. 2018, *A&A*, 616, A28
- Qin, Y., Marchant, P., Fragos, T., Meynet, G., & Kalogera, V. 2019, *The Astrophysical Journal*, 870, L18
- Quast, M., Langer, N., & Tauris, T. M. 2019, *A&A*, 628, A19
- Reig, P. 2011, *Ap&SS*, 332, 1
- Repetto, S., Davies, M. B., & Sigurdsson, S. 2012, *MNRAS*, 425, 2799
- Repetto, S., Igoshev, A. P., & Nelemans, G. 2017, *MNRAS*, 467, 298
- Rosslove, C. K. & Crowther, P. A. 2015, *MNRAS*, 447, 2322
- Ruffert, M. 1999, *A&A*, 346, 861
- Scarcella, F., Gaggero, D., Connors, R., et al. 2020, *arXiv e-prints*, arXiv:2012.10421
- Schweickhardt, J., Schmutz, W., Stahl, O., Szeifert, T., & Wolf, B. 1999, *A&A*, 347, 127
- Shakura, N. I. & Sunyaev, R. A. 1973, *A&A*, 500, 33
- Shao, Y. & Li, X.-D. 2020, *The Astrophysical Journal*, 898, 143
- Shapiro, S. L. & Lightman, A. P. 1976, *ApJ*, 204, 555
- Shapiro, S. L. & Teukolsky, S. A. 1983, *Black holes, white dwarfs, and neutron stars: the physics of compact objects*
- Shara, M. M., Crawford, S. M., Vanbeveren, D., et al. 2020, *MNRAS*, 492, 4430
- Soker, N., Livio, M., de Kool, M., & Savonije, G. J. 1986, *MNRAS*, 221, 445
- Stevenson, S., Ohme, F., & Fairhurst, S. 2015, *ApJ*, 810, 58
- Sukhbold, T., Woosley, S. E., & Heger, A. 2018, *ApJ*, 860, 93
- Sundqvist, J. O., Owocki, S. P., & Puls, J. 2018, *A&A*, 611, A17
- Tsuna, D., Kawanaka, N., & Totani, T. 2018, *MNRAS*, 477, 791
- Uglicano, M., Janka, H.-T., Marek, A., & Arcones, A. 2012, *ApJ*, 757, 69
- van den Heuvel, E. P. J., Portegies Zwart, S. F., & de Mink, S. E. 2017, *MNRAS*, 471, 4256
- van der Hucht, K. A. 2001, *VizieR Online Data Catalog*, III/215
- van der Hucht, K. A. 2006, *A&A*, 458, 453
- Vanbeveren, D., De Donder, E., Van Bever, J., Van Rensbergen, W., & De Loore, C. 1998a, *New A*, 3, 443
- Vanbeveren, D., De Loore, C., & Van Rensbergen, W. 1998b, *A&A Rev.*, 9, 63
- Vanbeveren, D., Mennekens, N., Shara, M. M., & Moffat, A. F. J. 2018, *A&A*, 615, A65
- Vanbeveren, D., Mennekens, N., van den Heuvel, E. P. J., & Van Bever, J. 2020, *A&A*, 636, A99
- Vilhu, O., Kallman, T. R., Koljonen, K. I., & Hannikainen, D. C. 2021, *arXiv e-prints*, arXiv:2104.02305
- Vink, J. S., de Koter, A., & Lamers, H. J. G. L. M. 2001, *A&A*, 369, 574
- Vink, J. S. & Sander, A. A. C. 2021, *MNRAS*, 504, 2051
- Waters, L. B. F. M., van den Heuvel, E. P. J., Taylor, A. R., Habets, G. M. H. J., & Persi, P. 1988, *A&A*, 198, 200
- Wellstein, S. & Langer, N. 1999, *A&A*, 350, 148
- Wiktorowicz, G., Lu, Y., Wyrzykowski, Ł., et al. 2020, *ApJ*, 905, 134
- Willems, B., Henninger, M., Levin, T., et al. 2005, *ApJ*, 625, 324
- Wong, T.-W., Valsecchi, F., Fragos, T., & Kalogera, V. 2012, *ApJ*, 747, 111
- Wood, K. S., Meekins, J. F., Yentis, D. J., et al. 1984, *ApJS*, 56, 507
- Woosley, S. E. 2019, *ApJ*, 878, 49
- Woosley, S. E., Sukhbold, T., & Janka, H. T. 2020, *ApJ*, 896, 56
- Wyrzykowski, Ł. & Mandel, I. 2020, *A&A*, 636, A20
- Yalinewich, A., Beniamini, P., Hotokezaka, K., & Zhu, W. 2018, *MNRAS*, 481, 930
- Yamaguchi, M. S., Kawanaka, N., Bulik, T., & Piran, T. 2018, *ApJ*, 861, 21
- Yuan, F. & Narayan, R. 2014, *ARA&A*, 52, 529
- Zhao, X., Gou, L., Dong, Y., et al. 2021, *ApJ*, 908, 117
- Zucker, S., Mazeh, T., & Alexander, T. 2007, *ApJ*, 670, 1326

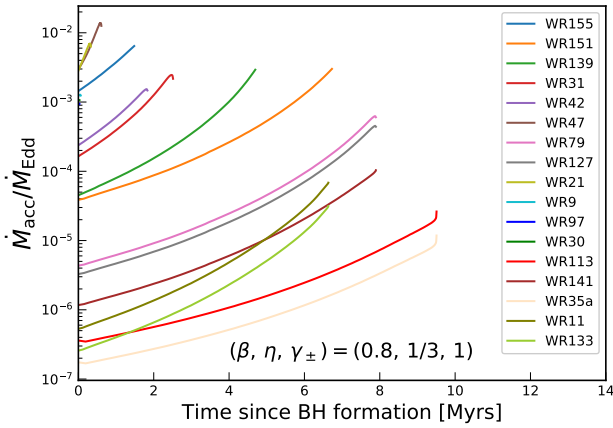
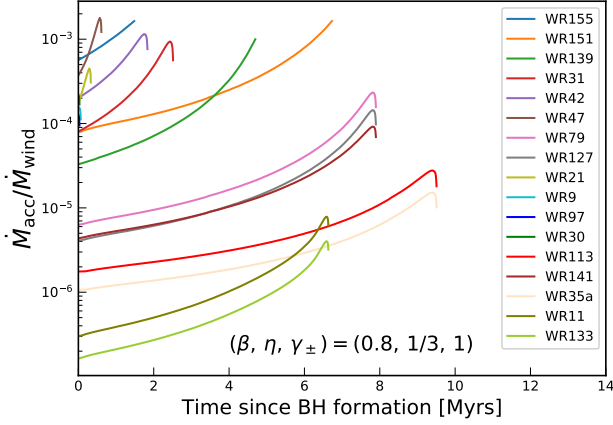


**Fig. A.1.** Comparison of mass accretion rate  $\dot{M}_{\text{acc}}$ , mass loss rate of the O star  $\dot{M}_{\text{wind}}$ , and Eddington accretion rate of the BH  $\dot{M}_{\text{Edd}}$  during the BH+O binary phase modelled from the 17 observed progenitor WR+O binaries, for  $(\beta, \eta, \gamma_{\pm}) = (0.8, 1/3, 1)$ . Upper and lower panels presents  $\dot{M}_{\text{acc}}/\dot{M}_{\text{wind}}$  and  $\dot{M}_{\text{acc}}/\dot{M}_{\text{Edd}}$  respectively. The colour coding in the legend denotes the 17 WR+O systems that are expected to form BH+O binaries.

## Appendix A: Mass accretion rate

Figure A.1 presents the comparison among the mass accretion rate, mass loss rate from the O star, and the Eddington accretion rate of the BH. The Eddington mass accretion rate is defined as

$$\dot{M}_{\text{Edd}} = \frac{L_{\text{Edd}} R_{\text{ISCO}}}{G M_{\text{BH}}}, \quad (\text{A.1})$$

where  $R_{\text{ISCO}}$  is the radius of the innermost stable circular orbit around BH,  $G$  is the gravitational constant,  $M_{\text{BH}}$  is the mass of BH, and  $L_{\text{Edd}}$  is the Eddington luminosity, evaluated by

$$L_{\text{Edd}} = L_{\odot} \frac{65335 M_{\text{BH}}}{1 + X M_{\odot}}, \quad (\text{A.2})$$

where  $X$  is the hydrogen abundance in the accreted material, which is expected to be the hydrogen abundance at the surface of donor star.

The upper panel shows that over 99% of wind material escape the BH+O system, which means the typical timescale of orbital evolution  $|a/\dot{a}|$  is longer than that of mass loss from O star  $|M_{\text{O}}/\dot{M}_{\text{O}}|$  (El Mellah et al. 2020a). The mass loss rate of O

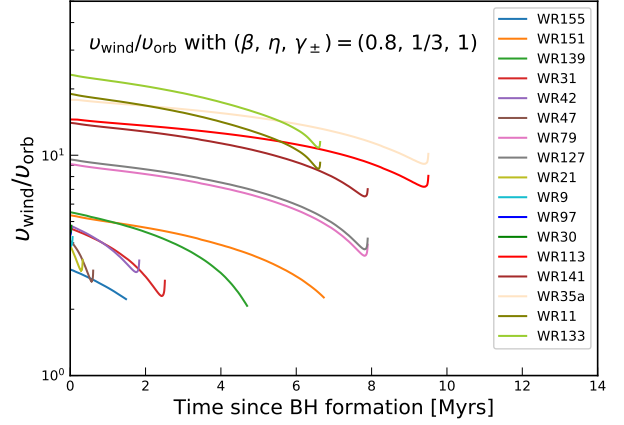


**Fig. B.1.** Evolution of the ratio of the O star wind velocity to the orbital velocity during the BH+O binary phase modelled from the 17 observed progenitor WR+O binaries, for  $(\beta, \eta, \gamma_{\pm}) = (0.8, 1/3, 1)$ . The colour coding in the legend denotes the 17 WR+O systems that are expected to form BH+O binaries.

star is about  $10^{-7} - 10^{-6} M_{\odot} \text{ yr}^{-1}$ . Therefore the orbital period of BH+O binary models can be safely treated as constant. The lower panel shows that the  $\dot{M}_{\text{acc}}$  is far below  $\dot{M}_{\text{Edd}}$ . Hence super-Eddington winds from the accretor does not occur in our models.

## Appendix B: Ratio of O star wind velocity to the orbital velocity

Figure B.1 presents the ratio wind velocity divided by orbital velocity  $v_{\text{wind}}/v_{\text{orb}}$ . The specific angular momentum obtained by SL76 only works in the fast-wind regime ( $v_{\text{wind}}/v_{\text{orb}} > 1$ ), which is consistent with our model that we always have  $v_{\text{wind}} > v_{\text{orb}}$ .

## Appendix C: Modifications on the disk formation criterion from Iben & Tutukov (1996)

Adopting the specific angular momentum Eq. (18) defined by Iben & Tutukov (1996) and updated wind velocity Eqs. (1) - (3), the ratio of  $R_{\text{disk}}/R_{\text{ISCO}}$  is

$$\frac{R_{\text{disk}}}{R_{\text{ISCO}}} = \frac{8 (R_{\text{O}}/a)^4}{3 (1+q)^2} \left( \frac{v_{\text{orb}}}{c} \right)^{-2} \left( 1 + \frac{v_{\text{wind}}^2}{v_{\text{orb}}^2} \right)^{-4} \gamma_{\pm}^{-1}, \quad (\text{C.1})$$

where  $q = M_{\text{O}}/M_{\text{BH}}$ . Comparing with Eq. (10), the efficiency parameter  $\eta$  for angular momentum accretion is replaced by  $(R_{\text{O}}/a)^4$ . For the WR+O binaries considered in this work,  $(R_{\text{O}}/a)^4$  is much smaller than  $\eta$ . Hence, we expect that this updated criterion Eq. (C.1) predicts fewer wind-fed BH HMXBs than that by Eq. (10).

Taking the  $\beta$  parameter for wind velocity law and the BH spin parameter  $\gamma_{\pm}$  to be equal to 1 in Eq. (C.1), the accretion disk formation criterion (Eq. 4) can be rewritten as

$$\frac{R_{\text{O}}}{a} \geq (2.6 \sqrt{1-\Gamma})^{8/7} \left( \frac{R_{\text{ISCO}}}{R_{\text{O}}} \right)^{1/7} (1+q)^{3/7} \left( 1 - \frac{R_{\text{O}}}{a} \right)^{8/7}. \quad (\text{C.2})$$

The wind velocity defined by Iben & Tutukov (1996) does not take into account the effect of the Eddington factor on the escape velocity and underestimates the ratio of the terminal velocity to the escape velocity. Further assuming that the binary mass

is equal to the mass of the non-compact companion, we obtain

$$\frac{R_{\text{disk}}}{R_{\text{ISCO}}} = \frac{8}{3} \left(\frac{R_{\text{O}}}{a}\right)^4 q^{-2} \left(\frac{v'_{\text{orb}}}{c}\right)^{-2} \left(\frac{v'_{\text{wind}}}{v'_{\text{orb}}}\right)^{-4}, \quad (\text{C.3})$$

where  $v'_{\text{orb}}$  is the orbital velocity assuming the binary mass is equal to the donor star mass and  $v'_{\text{wind}}$  is the wind velocity defined by Iben & Tutukov (1996), that is Eq. (20). Combining Eq. (4) and Eq. (C.3) lead to the disk formation criterion obtained by Iben & Tutukov (1996) (c.f. eq. 2 of V20),

$$\frac{R_{\text{O}}}{a} \geq \left(\frac{R_{\text{ISCO}}}{R_{\text{O}}}\right)^{1/7} q^{3/7} \left(1 - \frac{R_{\text{O}}}{a}\right)^{8/7}, \quad (\text{C.4})$$

which makes the disk formation much easier than Eq. (C.2). For example, in the BH+O model corresponding to WR 155, with  $\Gamma = 0.16$  and  $q = 2.5$  at the BH formation time, taking  $\gamma_{\pm} = 1$ ,  $\beta = 0.8$ , and the typical O star wind velocity reduces the ratio of  $R_{\text{disk}}/R_{\text{ISCO}}$  obtained from Eq. (C.1) by three orders of magnitude in comparison to that predicted from Eq. (C.3).